# Ion Channel Activity Assay by Planar Lipid Bilayer System

A detection of glucose-release activity from the liposome assay has suggested that our PEP-4 peptide is capable of forming a pore on the unilamelar lipid vesicle. A further investigation for a pore-forming activity of this peptide was performed on a planar lipid bilayer (PLB) system. Even through the setup and sample preparation for PLB experiment is complicated, but the experimental results can give a number of qualitative and quantitative data enough to describe for the ion channel property of the peptide. In our PLB experiment, we performed both symmetrical and asymmetrical assays for the purified PEP-4 peptide. While the results from a symmetrical system can be used to determine a conductance value that is specific for each ion channels, asymetrical system can reveal whether the channels are cation or anion selective.

A general PLB system contains two solution chambers, *cis* and *trans*, connected to each other through a small aperture painted with a lipid film. Our symmetrical system was filled with 150 mM KCl in both chambers, while the asymmetrical system was filled with 450 and 150 mM KCl in *cis* and *trans* chambers respectively. The command potentials were applied through small electrodes located inside the two chambers and electrical current was monitored for various potentials.

#### Symmetrical planar lipid bilayer experiments

Planar lipid bilayer experiment in symmetrical mode was performed to deduce the channel conductance. This parameter represents a characteristic value of the pore on lipid membrane. The results were obtained and depicted as a plot between the current observed versus progressive time period (Figure 12 to Figure 20). Our observation period for baseline experiment at 0 milivolt of applied potential was set 30-45 minutes to test for lipid membrane stability. Data derived from experiments with applied potentials from –100 to + 100 millivolts were collected for 60,000 to 100,000 milliseconds on a computer and only 2,000 milliseconds were shown in the figures.

# Jon channel assay at 0 millivolt

At the starting condition, a command potential of 0 millivolts was applied to the electrodes and the current signal was monitored against time for more than 45 minutes. The current was detected at the zero value as an indication for no channel activity. This condition was then used as a reference or baseline condition for other experiments.

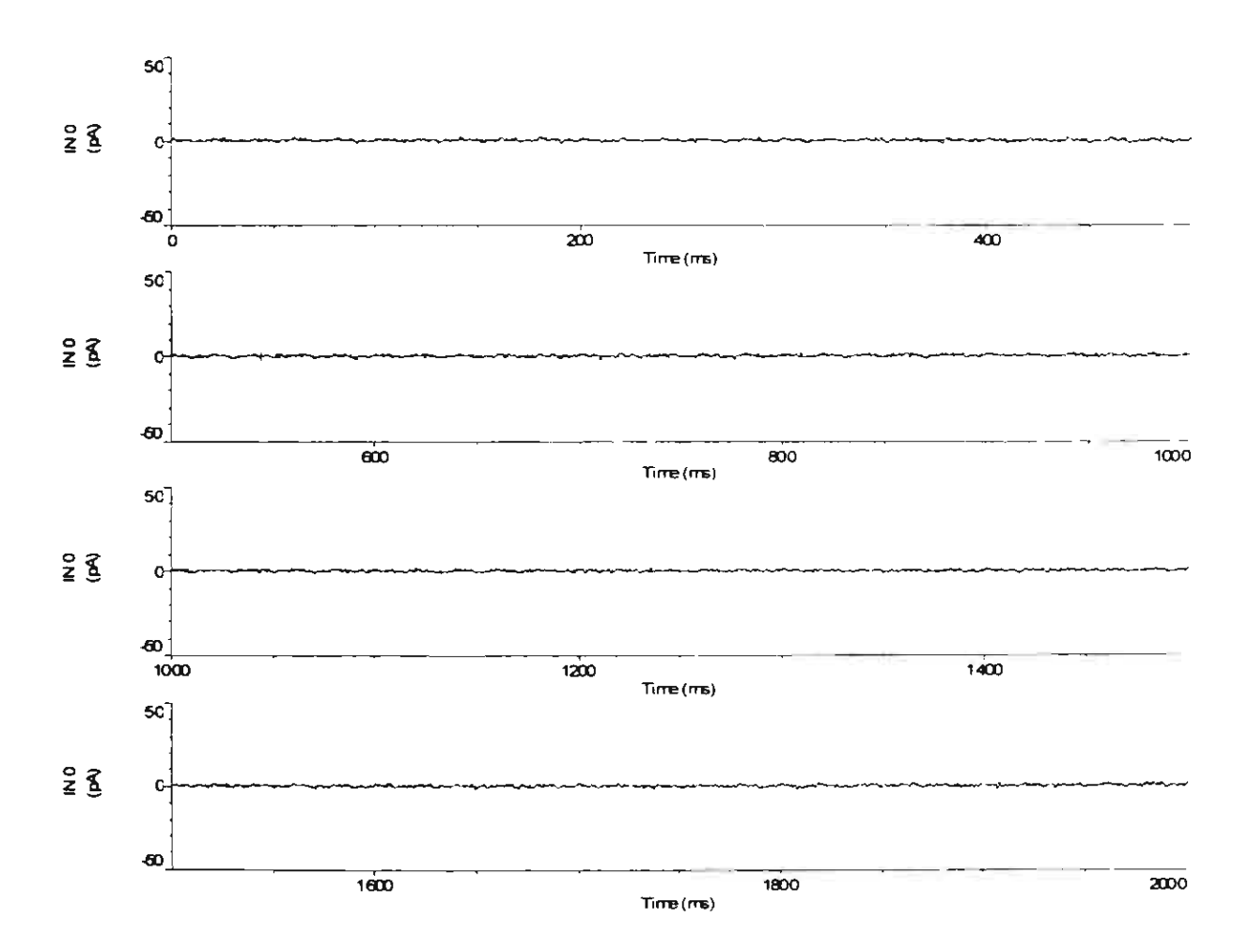


Figure 12: A plot between current and time obtained from planar lipid bilayer experiment at applied command potential of 0 millivolt. The time period shown is from 0 to 2000 milliseconds.

#### Ion channel assay at -100 millivolts

When a command potential of -100 millivolt was applied to the, we found a current jump from zero to a negative current signal. Signal analysis by AXOFit software gave a current value of -22.2 picoamperes. It is suggested that the channel activity were established on the membrane allowing ions to pass across and generate electrical current. The stability of the current indicated that the channel was in open state at all times.

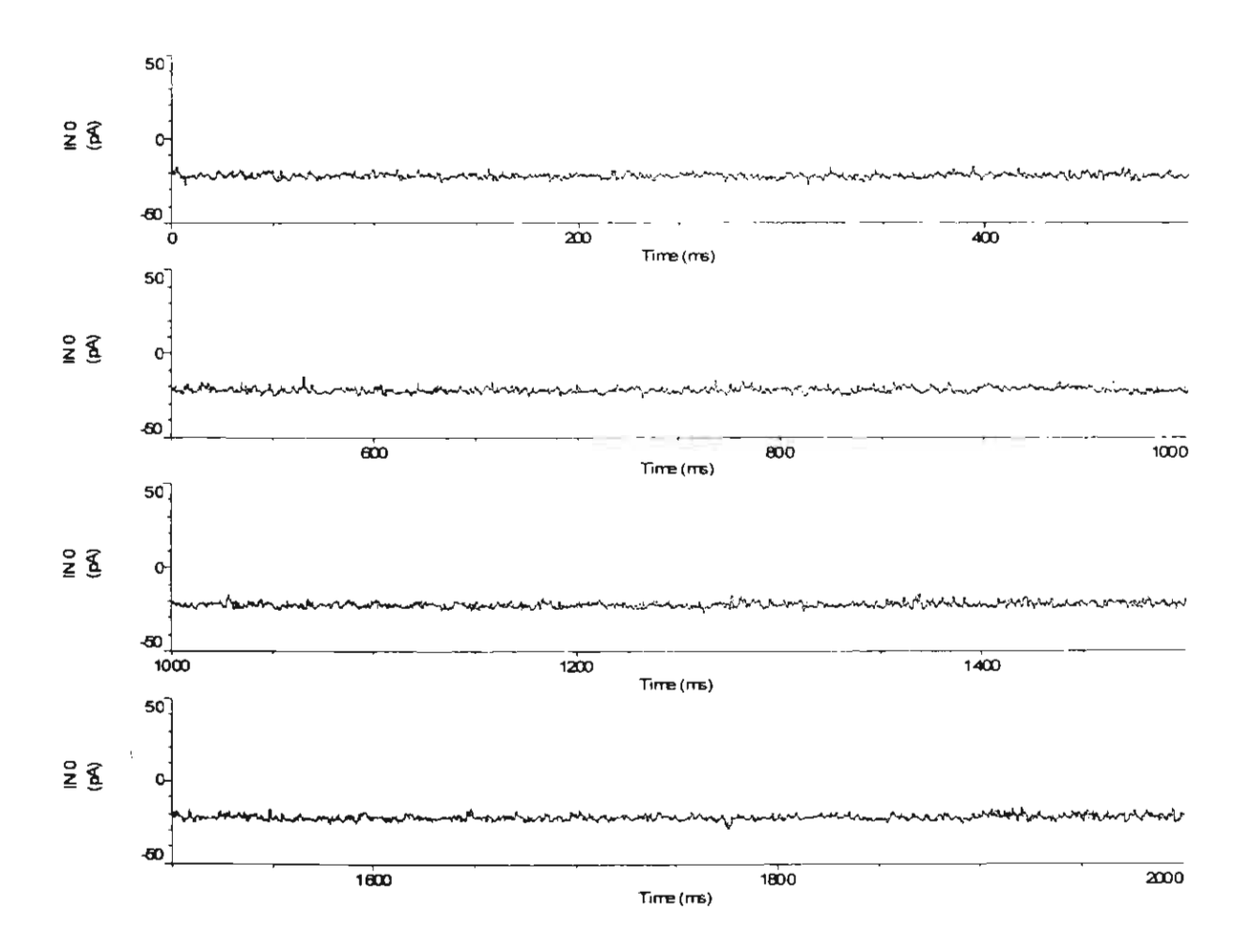


Figure 13: A plot between current and time obtained from planar lipid bilayer experiment at applied command potential of -100 millivolts. The time period shown is from 0 to 2000 milliseconds.

#### Ion channel assay at +100 millivolts

When a command potential of +100 millivolts was applied to the electrodes, we found a current jump from a negative to a positive current signal. Signal analysis by AXOFit software gave a current value of +18.1 picoamperes. It was suggested that there was an ion channel activity on the membrane. The current signal was found with a numbers of square jumps down to zero current indicating a transition from an opened to a closed state. However the open states were predominant than the closed state.

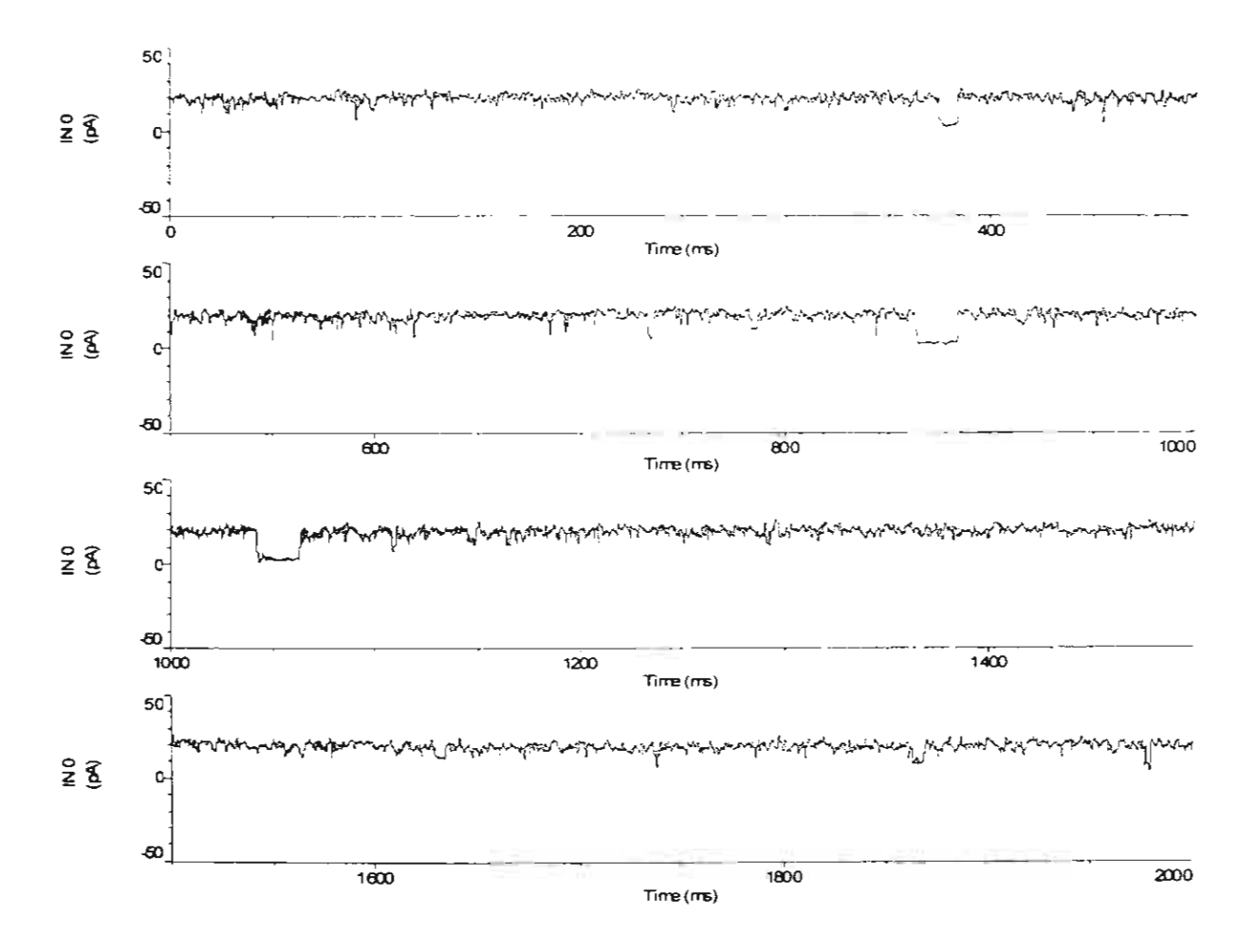
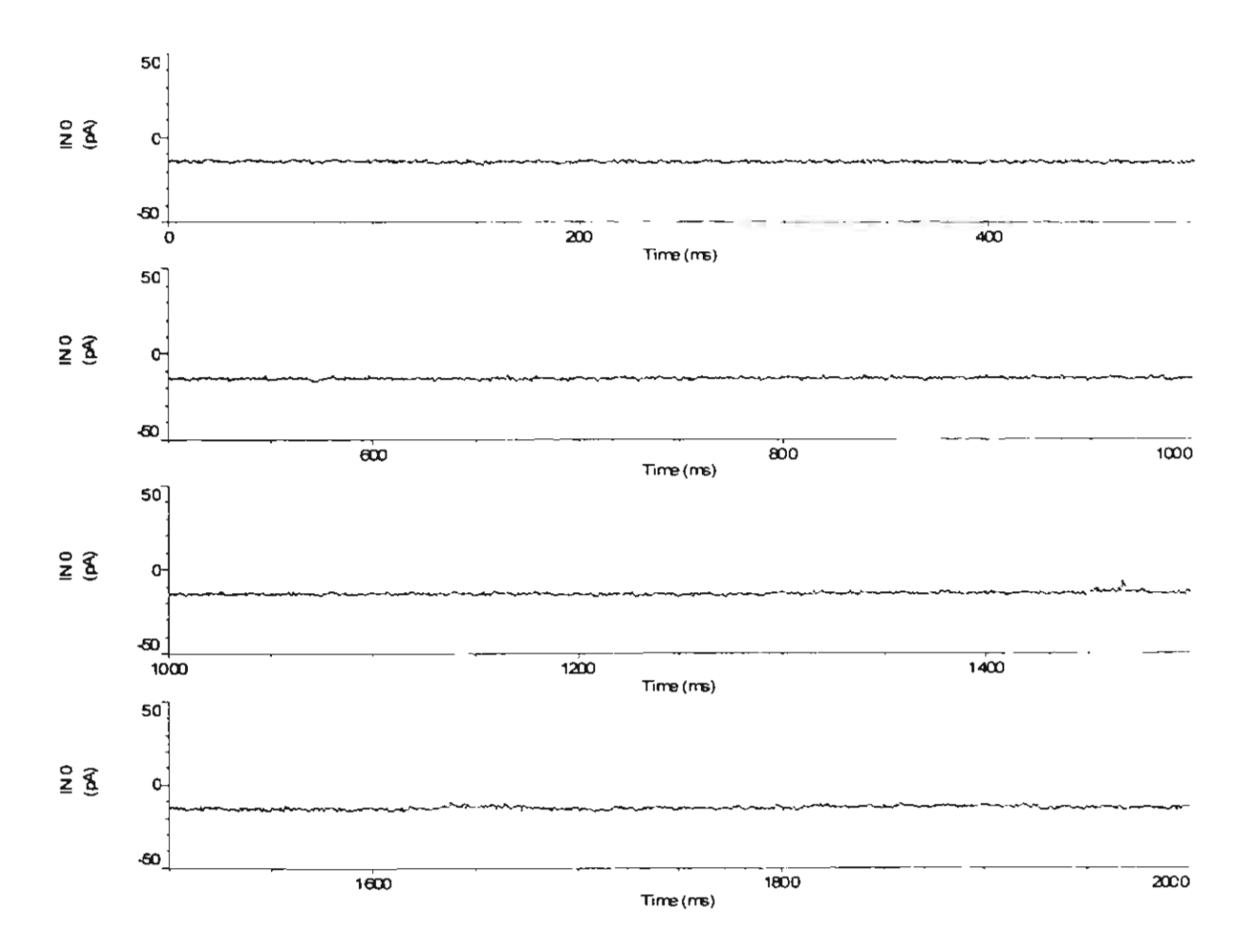


Figure 14: A plot between current and time obtained from planar lipid bilayer experiment at applied command potential of +100 millivolts. The time period shown is from 0 to 2000 milliseconds.

## Ion channel assay at -80 millivolts

When a command potential of -80 millivolts was applied to the electrodes, we found a current jump to a negative current signal. Signal analysis gave a current value of -14.2 picoamperes. This data suggested a channel activity on the membrane. The current signal was stable on the negative mode indicating an open state of channel.



**Figure 15:** A plot between current and time obtained from planar lipid bilayer experiment at applied command potential of -80 millivolts. The time period shown is from 0 to 2000 milliseconds.

#### Ion channel assay at +80 millivolts

When a command potential of -80 millivolts was applied to the electrodes, we found a current jump to a positive current signal. Signal analysis gave a current value of +11.3 picoamperes. This data demonstrated a channel activity on the membrane. The current signal was found to have square jumps back to zero current frequently showing a defined transition between open and close states of the channels

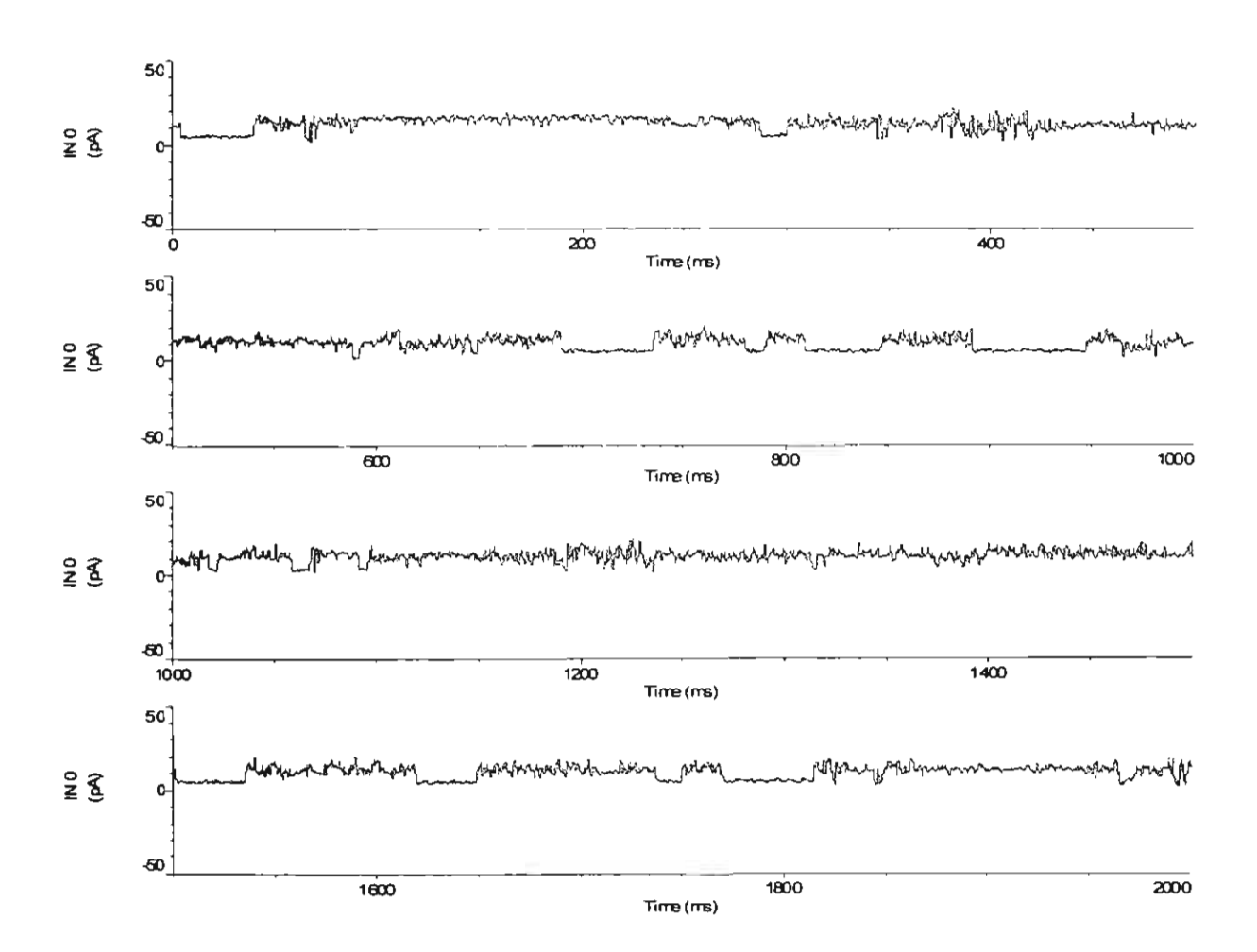
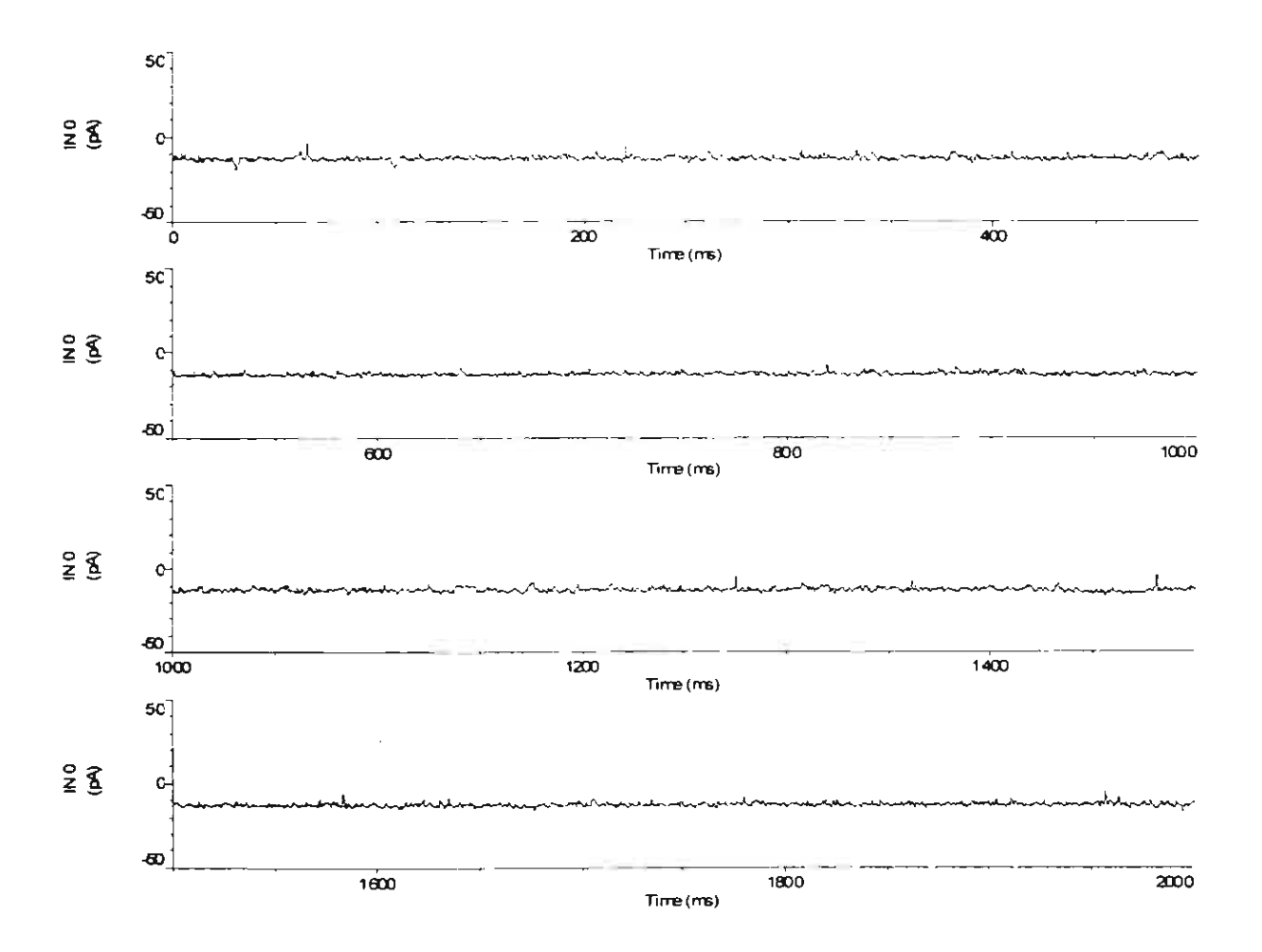


Figure 16: A plot between current and time obtained from planar lipid bilayer experiment at applied command potential of +80 millivolts. The time period shown is from 0 to 2000 milliseconds.

## Ion channel assay at -60 millivolts

After a command potential of -60 millivolts was applied to the system, we found a current jump to a negative current signal. Signal analysis gave a current value of -12.8 picoamperes. It was an indication for the channel activity on the membrane. The current signal was found with no square jumps back to the zero current revealing that the channels were in the open state.



**Figure 17:** A plot between current and time obtained from planar lipid bilayer experiment at applied command potential of -60 millivolts. The time period shown is from 0 to 2000 milliseconds.

# Ion channel assay at +60 millivolts

When a command potential of +60 millivolts was applied to the system, we found a current jump to a positive signal. Signal analysis yielded a current value of +11.0 picoamperes. It was an indicator for the channel activity on the membrane. The current signal was found to have no square jumps back to zero current revealing that the channel was in an open state.

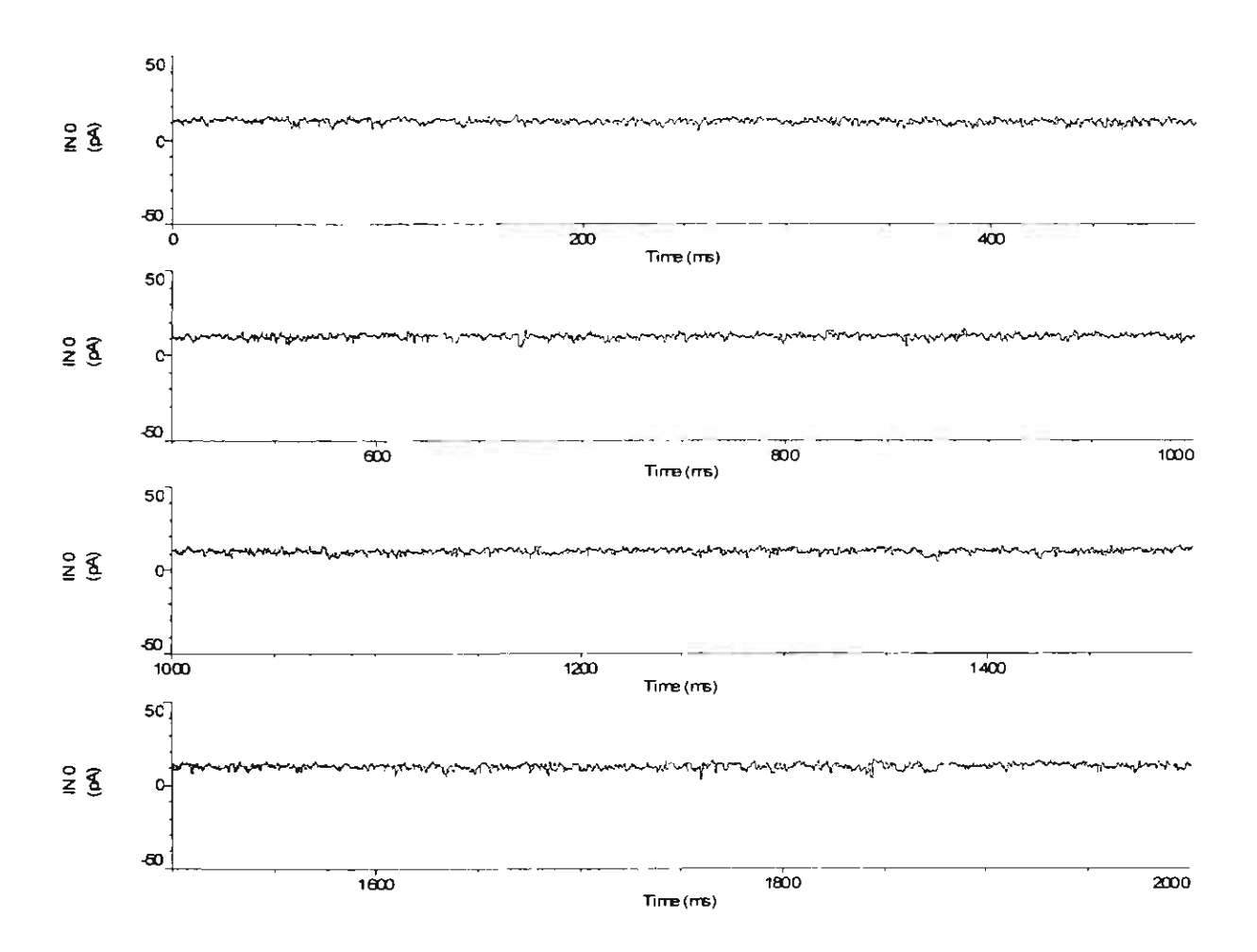


Figure 18: A plot between current and time obtained from planar lipid bilayer experiment at applied command potential of +60 millivolts. The time period shown is from 0 to 2000 milliseconds.

### Ion channel assay at -40 millivolts

A command potential of -40 millivolts applied to the system had led to a current jump to a negative signal. Signal analysis gave a current value of -8.4 picoamperes. It was an indication for the channel activity on the membrane. The current signal was found with a few square jumps back to the zero current showing a transition from open to close state. However the open state were much more predominated than the closed state.

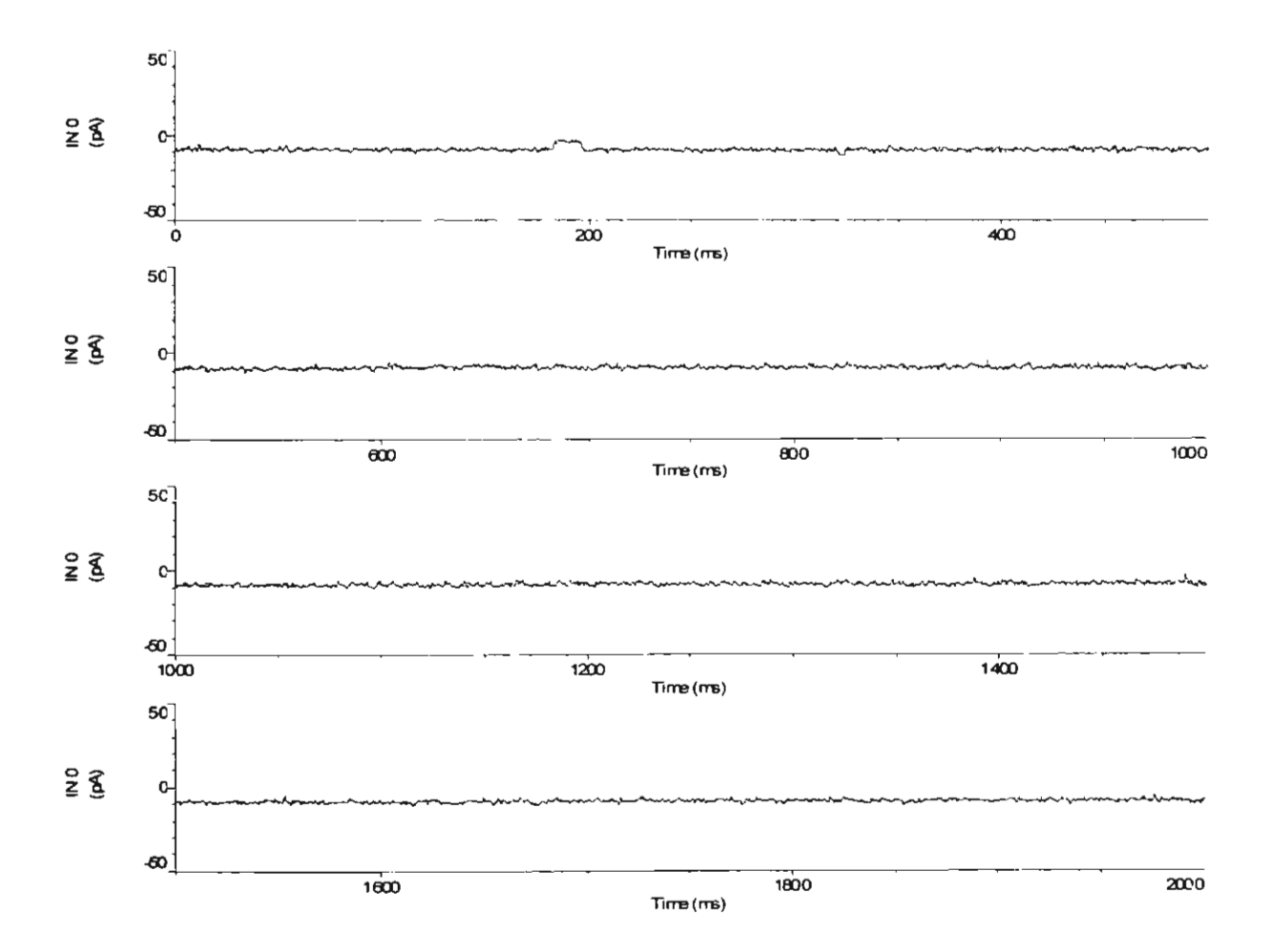


Figure 19: A plot between current and time obtained from planar lipid bilayer experiment at applied command potential of -40 millivolts. The time period shown is from 0 to 2000 milliseconds.

## Ion channel assay at +40 millivolts

After a command potential of +40 millivolts was applied to the system, we found a current jump to a negative current signal. Signal analysis yielded a current value of +7.0 picoamperes. It was an indication for the channel activity on the membrane. The current signal was found with no square jumps back to the zero showing open state of channel.

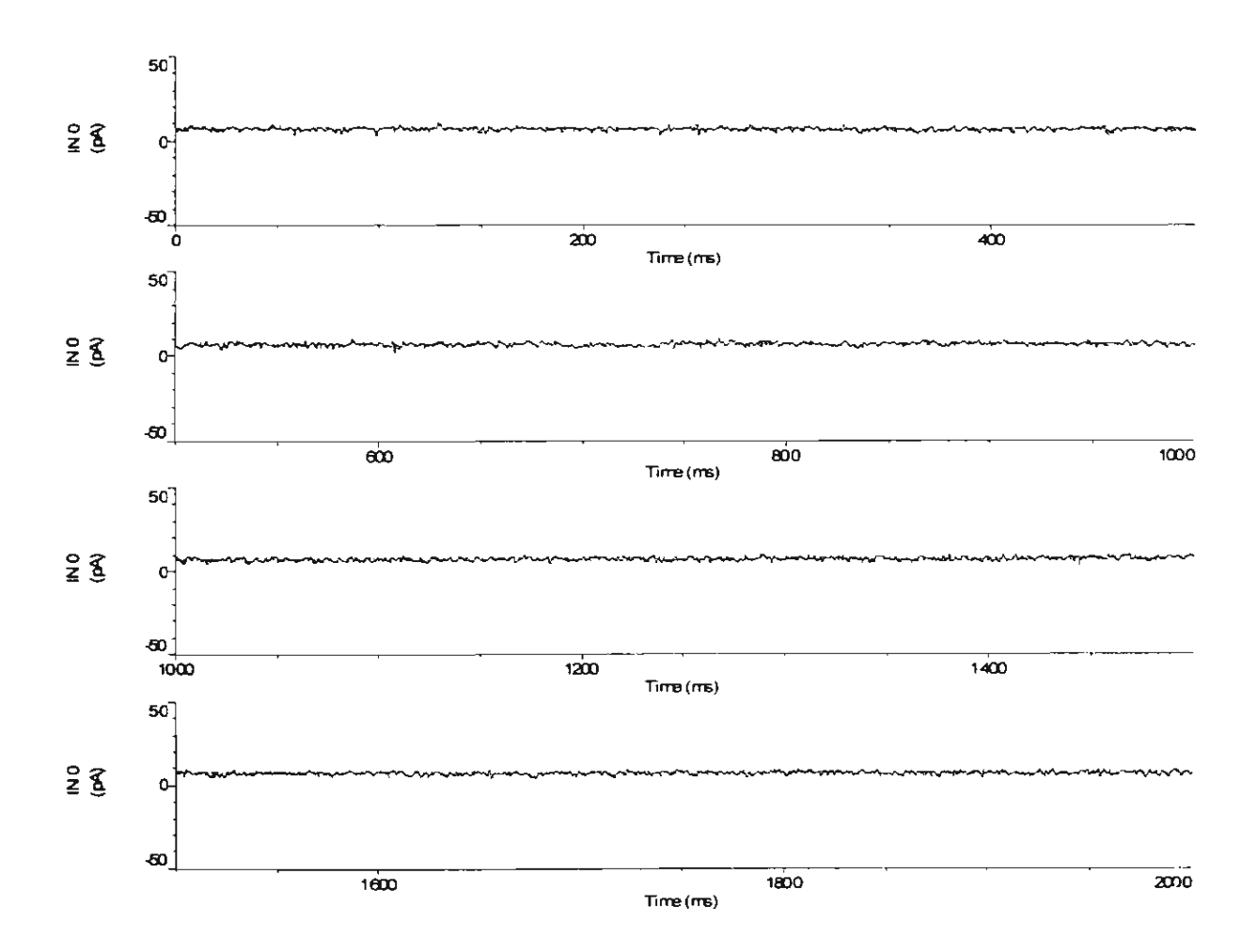


Figure 20: A plot between current and time obtained from planar lipid bilayer experiment at applied command potential of +40 millivolts. The time period shown is from 0 to 2000 milliseconds.

Based upon the zero current detected for the baseline at 0 millivolt potential, the nonzero current detected for all cases with applied potentials from -100, -80, -60, -40, +40, +60, +80, +100 millivolts indicated an ion channel activity of the PEP-4 peptide. The sign of detected currents were found to be corresponding to the sign of applied potentials. We found several square jumps of current to zero ampere and back to their stable values in several conditions (for +100, +80, and +60 mV potentials). These current jumps represent a rapid transition between an open state (nonzero current) and close state (zero current). However the channel observed in our experiments were found to spend most of their time in an open state.

The PLB experiment in symmetrical mode has allowed us to determine a conductance for this ion channel via a plot of detected currents against applied potentials. According to Ohm's law a slope of this plot (I/V) is a reciprocal of resistance or defined as a conductance.

$$I/V = 1/R = Conductance$$

The coordinates for the I and V plot was listed in table 5, corresponding to detected currents in picoamperes and the applied potentials in millivolts.

Applied Potentials	Detected Currents
(mV)	(pA)
0	0.0
- 100	- 22.2
+ 100	+ 18.1
- 80	- 14.2
+ 80	+ 11.3
- 60	- 12.8
+ 60	+ 11.0
- 40	- 8.4
+ 40	+ 7.0

Table 5: Detected current values at various applied potentials obtained from symetric planar lipid bilayer experiment.

A plot of I against V has produced a linear relationship with correlation factor ( $R^2$ ) of 0.988. The slope determined from the fitted equation, I = 0.188V – 1.133 was 188 pS. This means that the ion channel produced from PEP-4 peptide has a characteristic conductance of 188 pS.

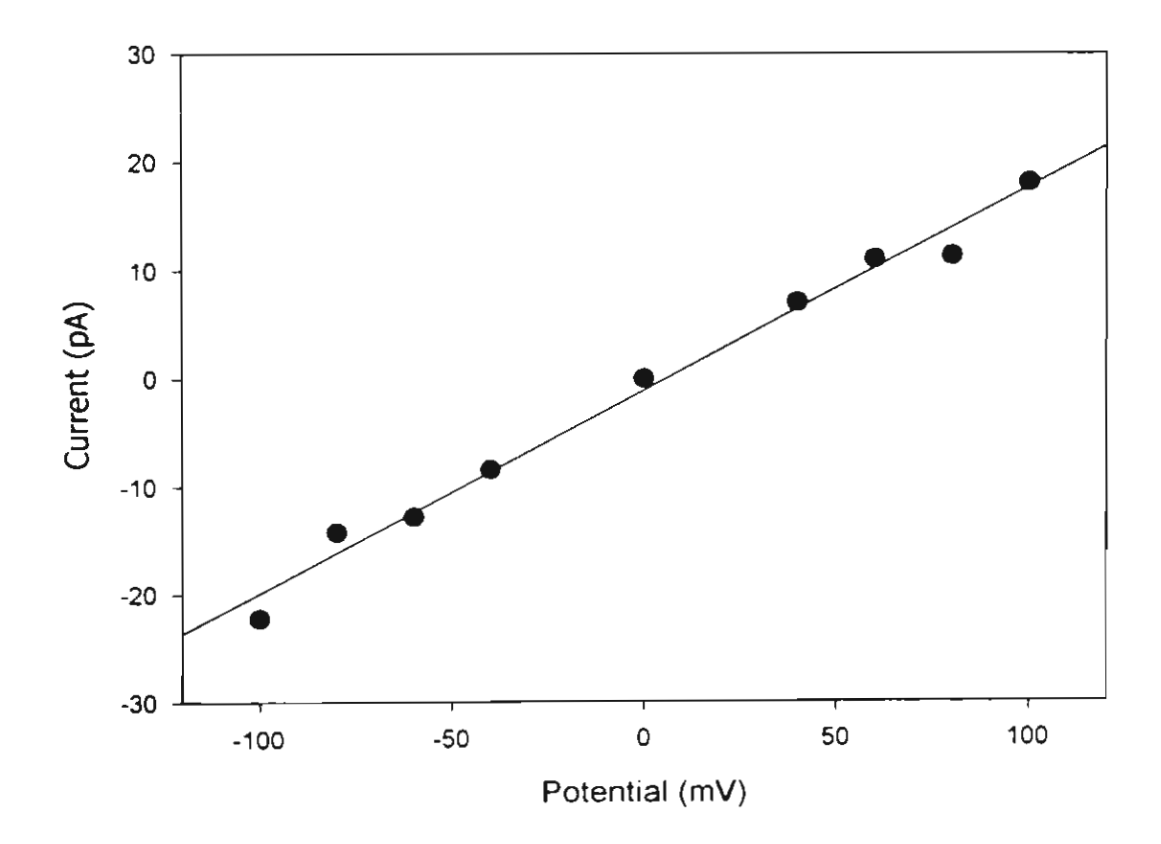


Figure 21: A plot between applied potentials and detected currents obtained from symmetrical planar lipid bilayer experiment.

# Asymmetrical planar lipid bilayer experiments

We continued the experiment on planar lipid bilayer in an asymmetrical mode aiming to determine the type of ion channel. *Cis* chambers was filled with a higher concentration of KCl (450 mM against 150 mM) and the modulated activity was monitored at various potentials. The data were depicted as a plot between detected currents and progressive time periods (Figure 22 to Figure 29)

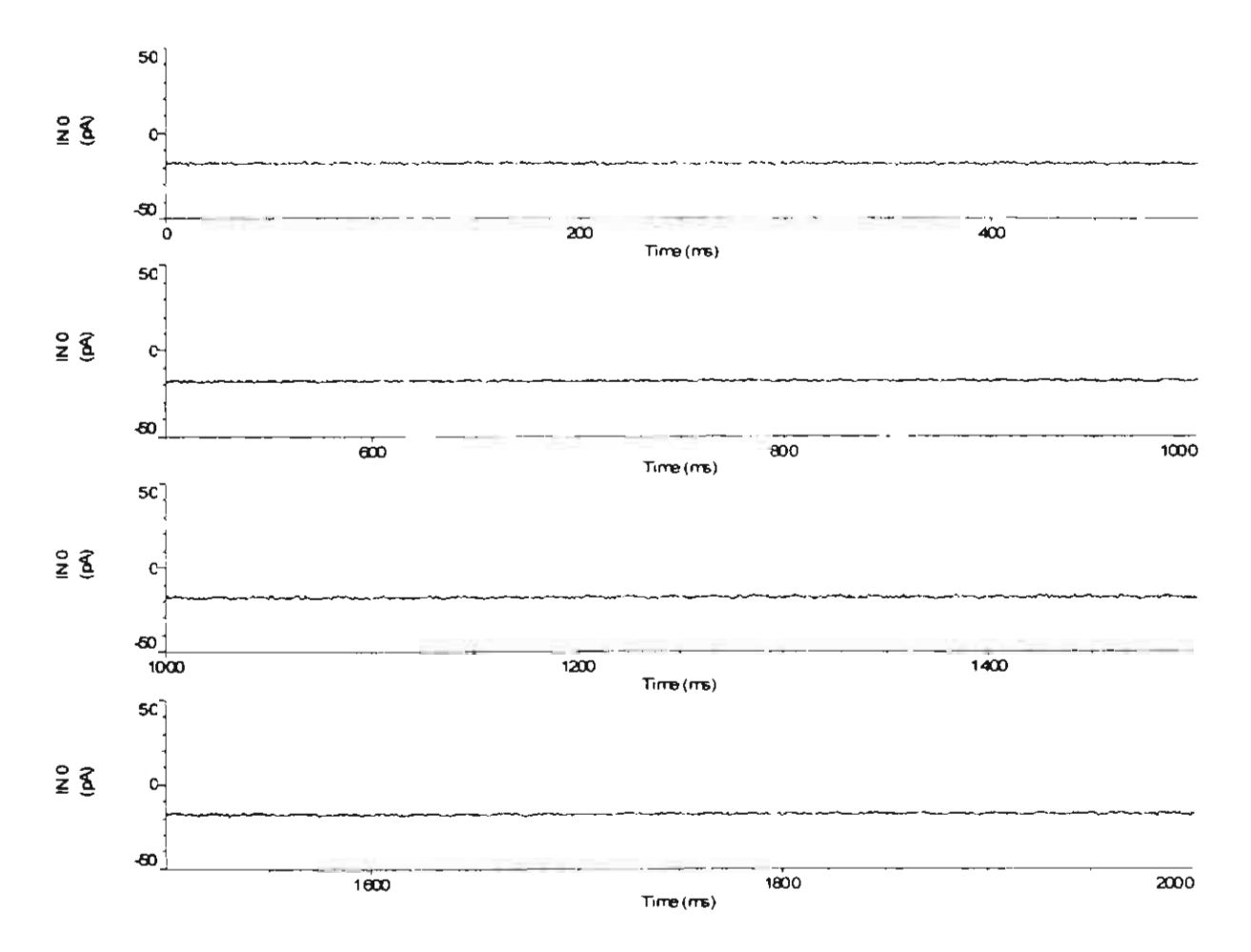


Figure 22: A plot between current and time for asymetric planar lipid bilayer experiment at applied potential -80 millivolts. Signal analysis gave the current value at -18.5 picoamperes.

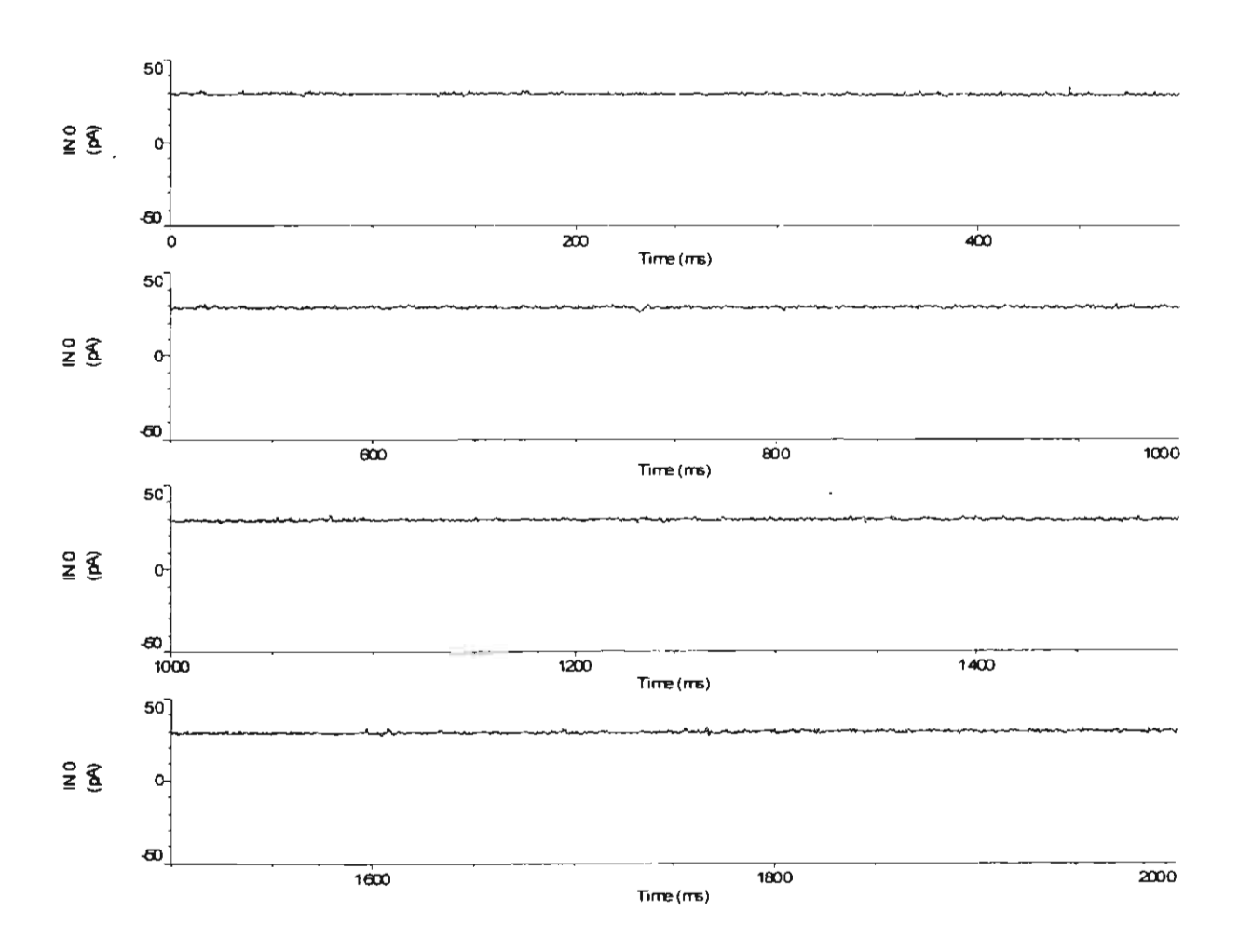


Figure 23: A plot between current and time for asymetric planar lipid bilayer experiment at applied potential +80 millivolts. Signal analysis gave the current value at +29.0 picoamperes.

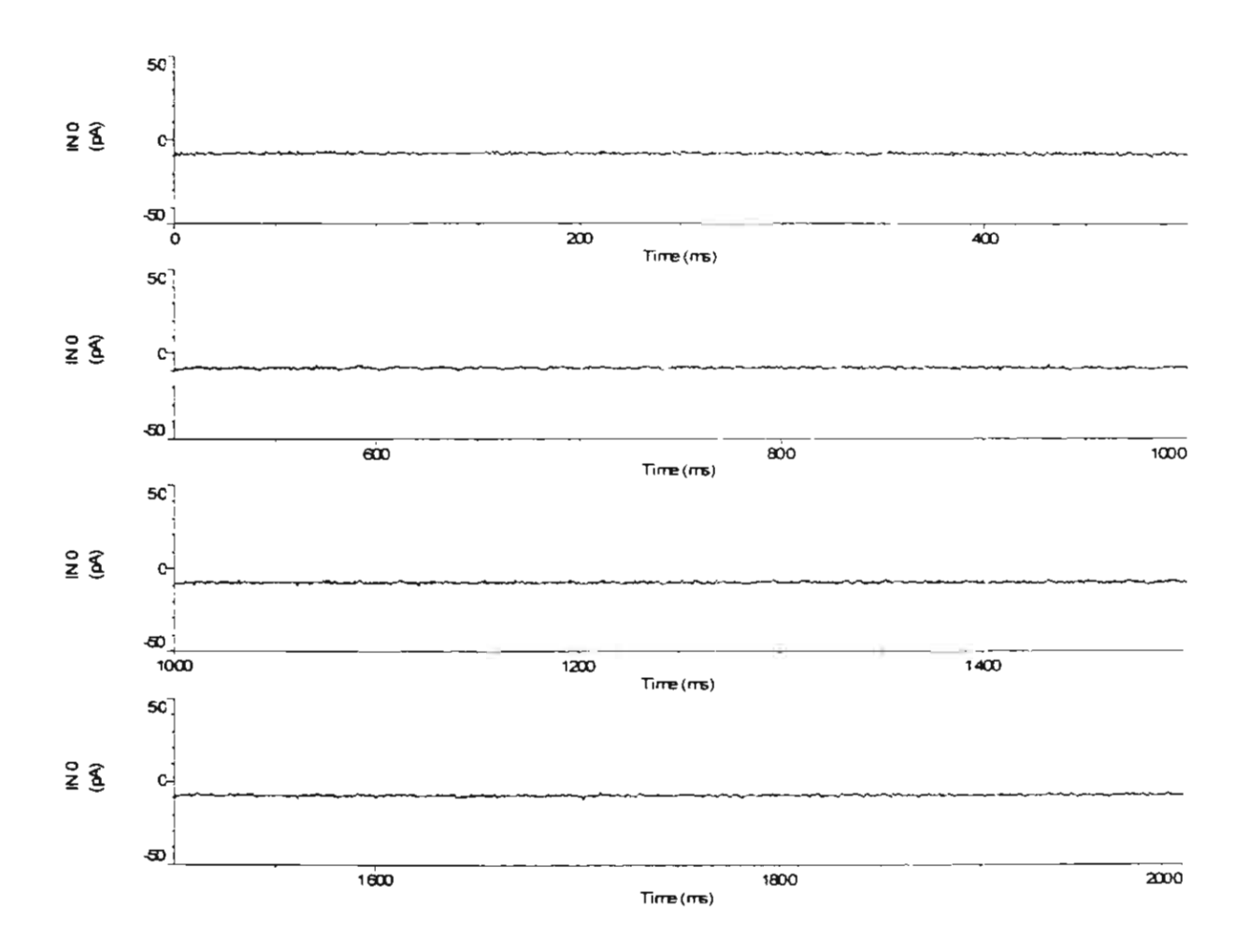


Figure 24: A plot between current and time for asymetric planar lipid bilayer experiment at applied potential -50 millivolts. Signal analysis gave the current value at -8.4 picoamperes.

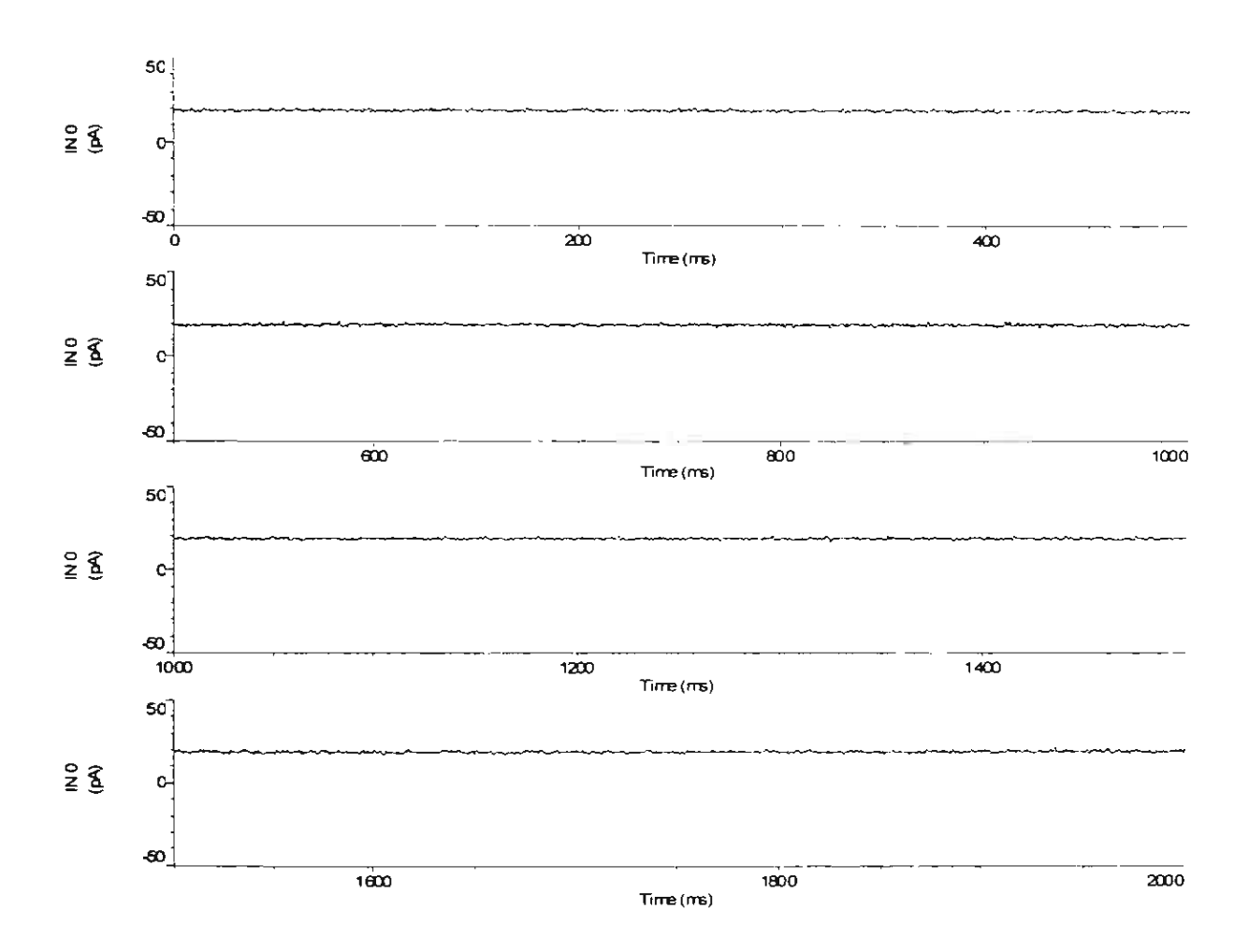


Figure 25: A plot between current and time for asymetric planar lipid bilayer experiment at applied potential +50 millivolts. Signal analysis gave the current value at +18.5 picoamperes.

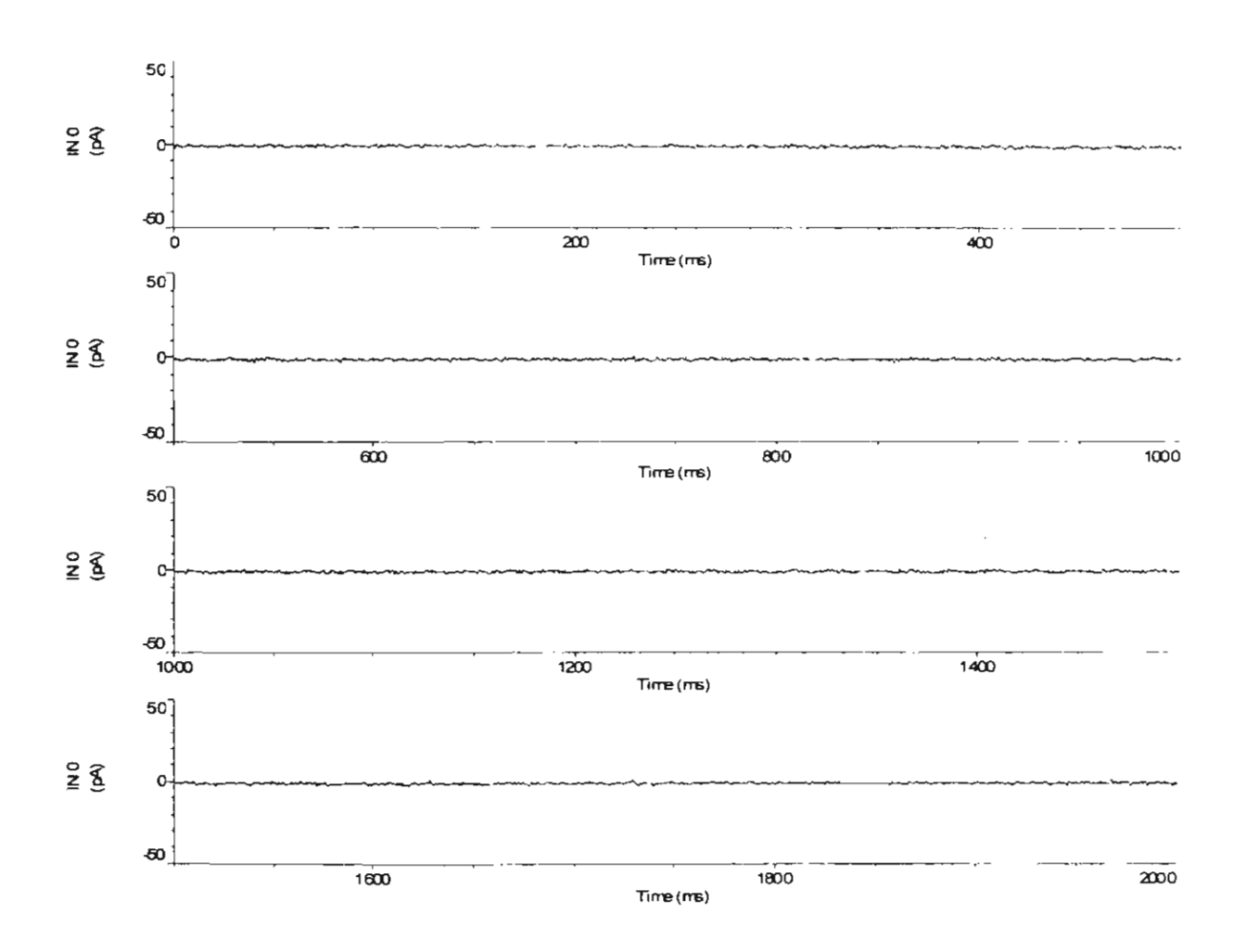


Figure 26: A plot between current and time for asymetric planar lipid bilayer experiment at applied potential -20 millivolts. Signal analysis gave the current value at -0.9 picoamperes.

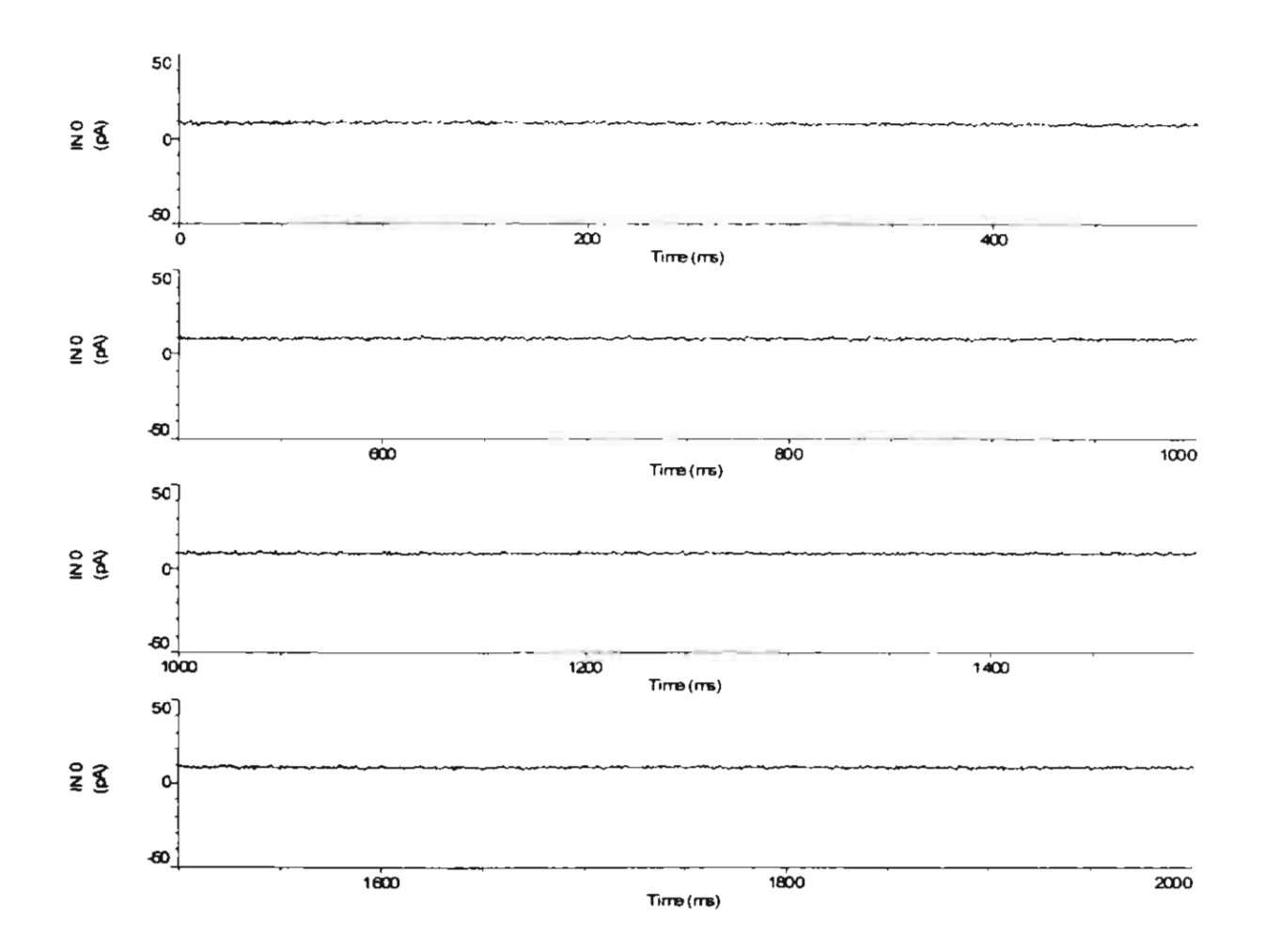


Figure 27: A plot between current and time for asymetric planar lipid bilayer experiment at applied potential +20 millivolts. Signal analysis gave the current value at +9.6 picoamperes.

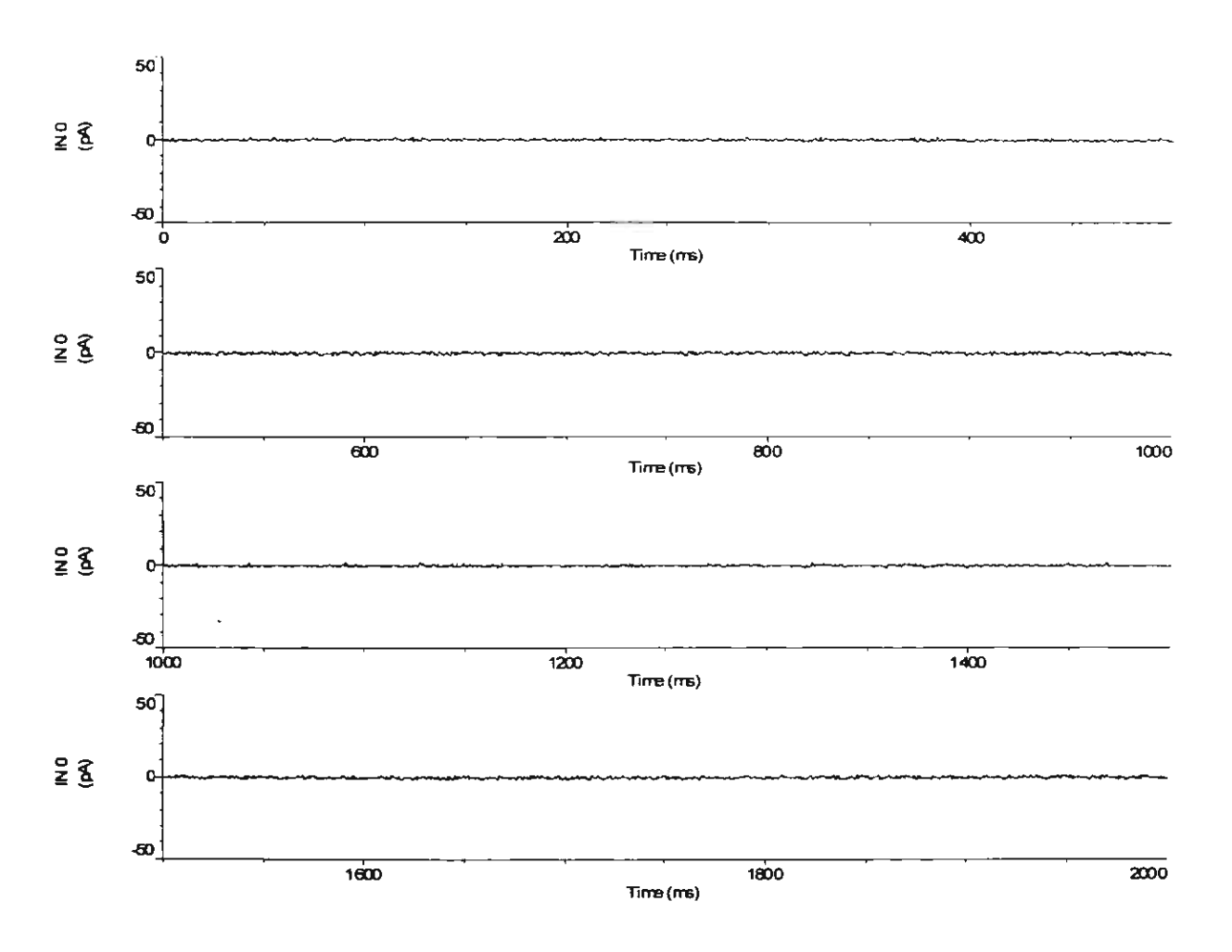


Figure 28: A plot between current and time for asymetric planar lipid bilayer experiment at applied potential -18 millivolts. Signal analysis gave the current value at -0.4 picoamperes.

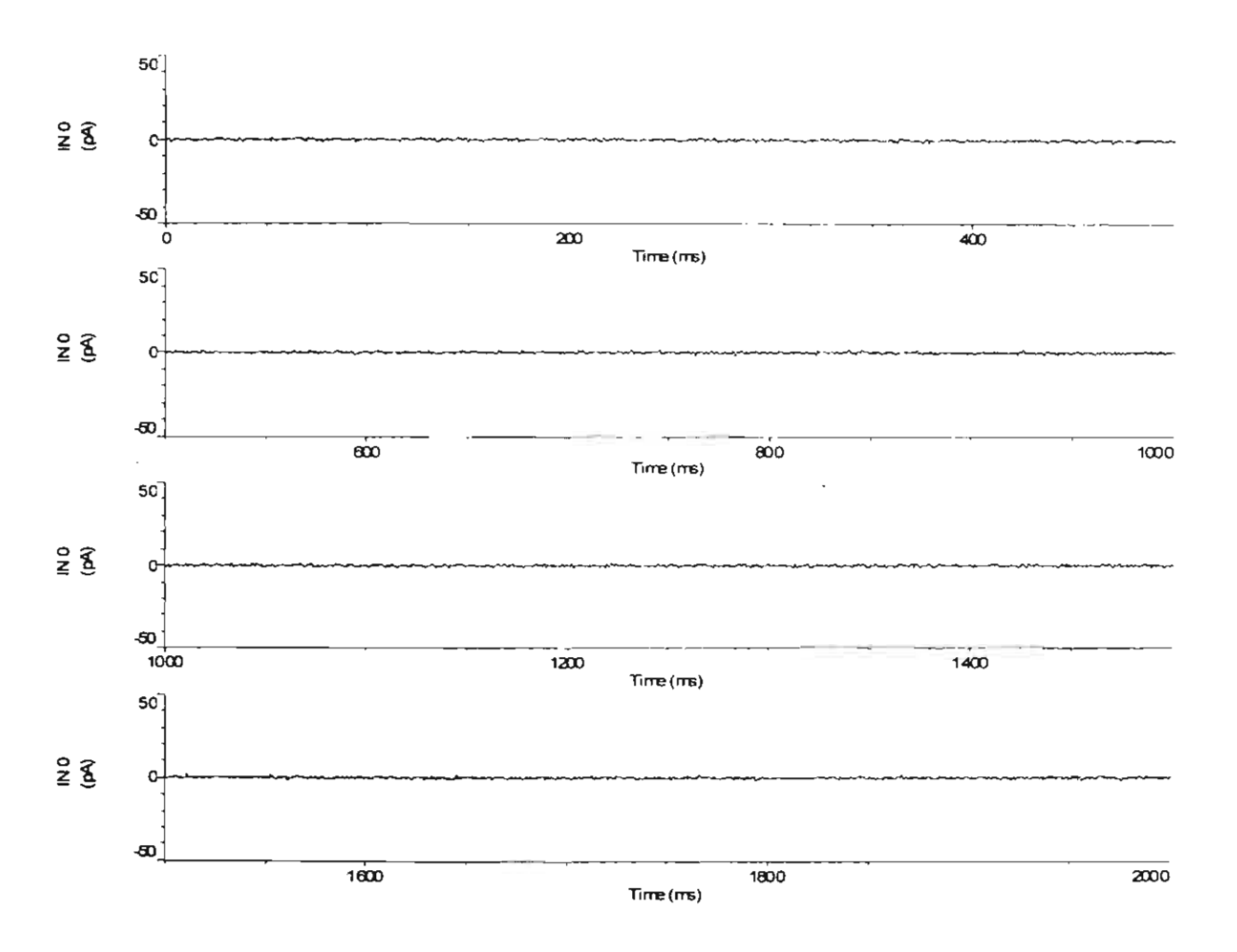


Figure 29: A plot between current and time for asymetric planar lipid bilayer experiment at applied potential -16 millivolts. Signal analysis gave the current value at +0.2 picoamperes.

From the detected currents observed in various applied potential conditions, we can summarize the data as listed in Table 6.

Applied Potentials (mV)	Detected Currents (pA)
- 80	- 18.5
+ 80	+ 29.0
- 50	- 8.4
+ 50	+ 18.5
- 20	- 0.9
+ 20	+ 9.6
- 18	- 0.4
- 16	+ 0.2

Table 6: Detected current values at various applied potentials obtained from asymetric planar lipid bilayer experiment.

A plot of detected currents against applied potentials has produced a linear relationship between the two variables (Figure 30). Curve fitting was performed with good correlation factor (R<sup>2</sup>) of 0.997 and fitted equation of I = 0.288V + 4.862. Unlike a symmetrical mode, the asymmetrical experiment will not give a zero current at applied potential of 0 mV. To get a zero current in this system, there must be some potential applied for a reversal of an ion flow. This reversed potential can be determined from the fitted equation by substitution of I with zero. A reversed potential obtained for our PEP-4 peptide was -16.88 mV. Since a negative potential is needed to inhibit ion flow of K+ ion, this channel is classified as a cation-selective channel.

From our planar lipid bilayer experiment the results revealed that the pore or channel can be generated on the artificial membrane by PEP-4 peptide. The characteristics of this channel are the conductance of 188 pS and selecting for cation. However other morphology and properties of this channel can not be characterized by planar lipid bilayer experiment.

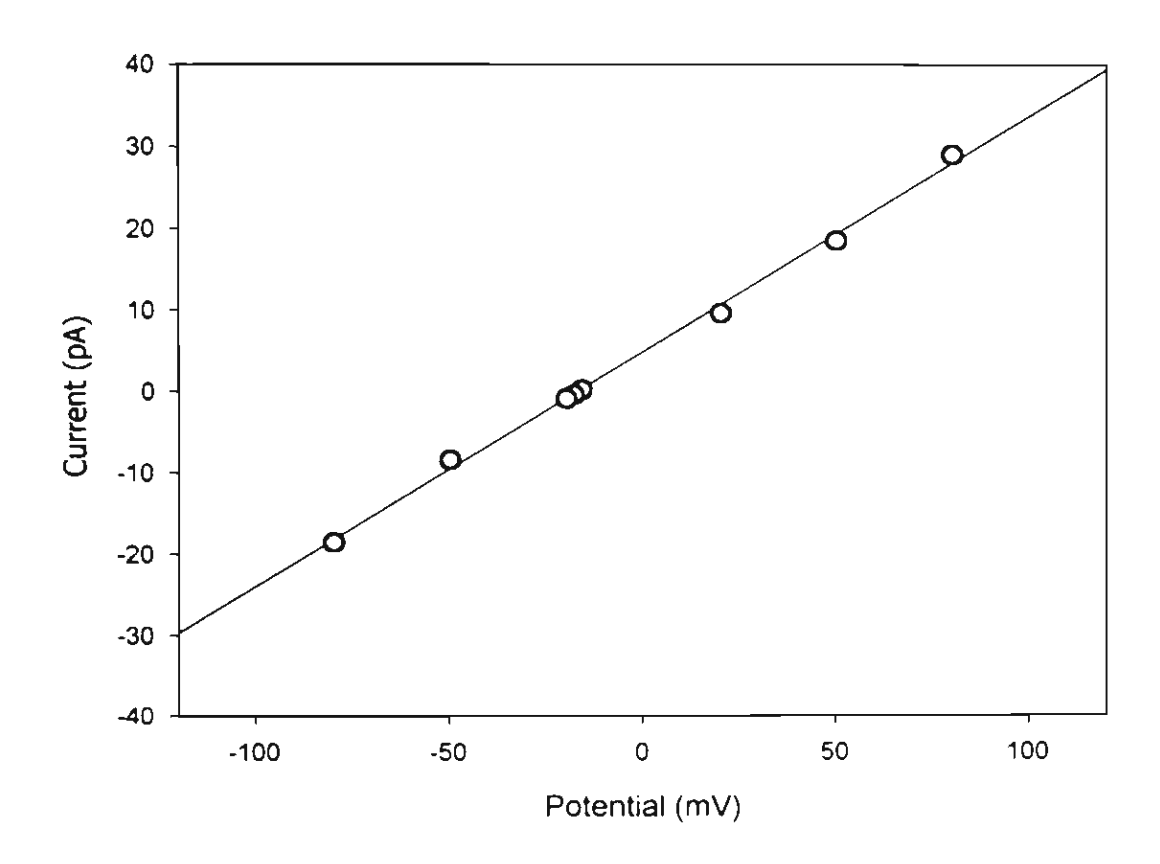


Figure 30: A plot between applied potentials and detected currents obtained from planar lipid bilayer experiment in asymmetrical mode.

# **Concluding Remarks**

We have demonstrated a process for *de novo* design for an alpha-helical peptide with pore-forming activity. The design strategy was based on the selection of amino acid residue of high helical propensity, the minimal length of helix for membrane insertion, and the amphipathicity containing one-third of hydrophobic surface. The designed peptide models were analyzed and showed comparable stability with known helical peptide and then synthesized by solid phase synthesis. Characterization of the purified peptides indicated an alpha helical structure as expected. We found one peptide, PEP-4 of sequence Acetyl-YALSLAATLLKEAASL-OH, is capable of releasing glucose entrapped in the liposome. Further characterization of this peptide on an artificial membrane using planar lipid bilayer gave a channel activity for cation permeability with 188 pS conductance.

This work has proved to be an accomplishment of peptide design strategy based on a simple structural concept. However the application of the design principle may not be the universal rule for definite prediction of structure and function. It has rather been employed as a valuable facilitating tool for structural prediction and for more understanding on the concept of protein and peptide structure and function.

#### References

- Aurora, R., Creamer, T. P., Srinivasan, R. & Rose, G. D. (1997) Local interaction in protein folding: Lessons from the alpha helix. *J. Biol. Chem.*, 272, 1413-1416.
- Blanco, F.J., Ortiz, A.R., & Serrano, L. (1997) Role of nonnative interaction in the folding of protein G B1 domain as inferred from the conformational analysis of the α-helix fragment. *Folding and Design* 2, 123-133.
- Chmielewski, J., & Lipton. M. (1994) The rational design of a highly stable amphiphilic helical peptides. *Int. J. Peptide Protein Res.* 44, 152-157.
- Choe, S., Bennett, M.J., Fujii, G., Curmi, P.M.G., Kantardjieff, A., Collier, R..J., & Eisenberg, D. (1992) The crystal structure of diphtheria toxin. *Nature* 357, 216-222.
- Cummings, C.E., Armstrong, G., Hodgman, T.C., & Ellar, D.J. (1994) Structural and functional studies of a synthetic peptide mimicking a proposed membrane inserting region of a Bacillus thuringiensis. *Mol. Membr. Biol.* 2, 87-92.
- Dolphin, G., & Baltzer, L. (1997) The pH-dependent tertiary structure of a designed helix-loop-helix dimer. *Folding and Design* 2, 319-330.
- Dieckmann, G., & DeGrado, W.F. (1997) Modeling transmembrane helical oligimers. *Curr. Opin. Struct. Biol.* 7, 486-494.
- Elkins, P., Bunker, A., Cramer, W.A., & Stauffacher, C.V. (1997) The crystal structure of the channel-forming domain of colicin E1. *Structure* 5, 443-458.
- Fairman, R., Chao, H.G., Lavoie, T.B., Villafranca, J.J., Matsueda, G.R. & Novotny, J. (1996) Design of heterotetrameric coiled coils: Evidence for increased stabilization by Glu-Lys ion pair interactions. *Biochemistry* 35, 2824-2829.
- Gazit, E., & Shai, Y. (1995) The assembly and organization of the  $\alpha$ 5 and  $\alpha$ 7 helices from the pore-forming domain of bacillus thuringiensis  $\delta$ -endotoxin. *J. Biol. Chem.* 270, 2571-2578.
- Grochulski, P., Masson, L., Borisova, S., Pusztai-Carey, M., Schwartz, J. L., Brousseau, R., & Cygler, M. (1995) Bacillus thuringiensis crylAa insecticidal toxin: crystal structure and channel formation. *J. Mol. Biol.* 254, 447-464.
- Gurunath, R., Beena, T.K., Adiga, P.R., & Balaram, P. (1995) Enhancing peptide antigenicity by helix stabilization. *FEBS Lett.* 361, 176-178.
- Haider, M.Z., & Ellar, D.J. (1989) Mechanism of action of Bacillus thuringiensis insecticidal delta-endotoxin: interaction with phospholipid vesicles. *Biochim. Biophys. Acta.* 978, 216-222.
- Kinsky, S.C. (1974) Preparation of liposomes and a spectrophotometric assay for release of trapped glucose marker. *Methods Enzymol.* 32, 501-513.
- Krittanai, C. & Johnson, W. C. (2000) Relative order of helical propensity of amino acids changes with solvent environment. *PROTEINS: Struct. Funct. & Genet.* 39, 132-141.
- Li, J., Carroll, J., & Ellar, D.J. (1991) Crystal structure of insecticidal δ-endotoxin from Bacillus thuringiensis at 2.5 A resolution. *Nature* 353, 815-821.
- Li, J., Koni, P.A., & Ellar, D.J. (1996) Structural of the mosquitocidal δ-endotoxin CytB from Bacillus thuringiensis sp. Kyushuensis and implications for membranes pore formation. *J. Mol. Biol.* 257, 129-152.
- Lumb, K.J., & Kim, P.S. (1995) A buried polar interaction imparts structural uniqueness in a designed heterodimeric coiled coil. *Biochemistry* 34, 8642-8648.
- Nagi, A., & Regan, L. (1997) An inverse correlation between loop length and the stability in a four-helix-bundle protein. *Folding and Design* 2, 67-75.

- Parker, M.W., & Pattus, F. (1993) Rendering a membrane protein soluble in water: A common packing motif in bacterial protein toxins. *Trends Biochem. Sci.* 18, 391-395.
- Parker, M.W., Postma, J.P.M., Pattus, F., Tucker, A.D., & Tsernoglou, D. (1992) Refine structure of pore-forming domain of colicin A at 2.4 A resolution. *J. Mol. Biol.* 224, 639-657.
- Parker, M.W., Pattus, F., Tucker, A.D., & Tsernoglou, D. (1989) Structure of the membrane-pore-forming fragment of colicin A. *Nature* 337, 93-96.
- Petosa, C., Collier, R.J., Klimpel, K.R., Leppla, S.H., & Liddington, R.C. (1997) Crystal structure of the anthrax toxin protective antigen. *Nature* 385, 833-838.
- Predki, P.F., & Regan, L. (1995) Redisigning the topology of a four-helix-bundle protein: monomeric rop. *Biochemistry* 34, 9834-9839.
- Schwartz, J.L., Garneau, L., Masson, L., Brousseau, R., & Rousseau, E. (1993)
  Lepidopteran-specific δ-endotoxin from Bacillus thuringiensis form cation- and anion-selective channels in planar lipid bilayers. *J. Membr. Biol.* 132, 53-62.
- Silverman, J.A., Mindell, J.A., Zhan, H., & Collier, R.J. (1994) Structure-function relationships in diphtheria toxin channels: I. Determining a minimal channel-forming domain. *J. Membr. Biol.* 137, 17-28.
- Song, L., Hobaugh, M.R., Shustak, C., Cheley, S., Bayley, H., & Gouaux, J.E. (1996) Structure of staphylococcus α-hemolysin, a heptameric transmembrane pore. Science 274, 1859-1866.
- Stellwagen, E., Park, S.H., Shalongo, W., & Jain, A. (1992) The contribution of residue ion pairs to the helical stability of a model peptide. *Biopolymers* 32, 1193-1200.
- Wiener, M., Freymann, D., Ghosh, P., & Stroud, R.M. (1997) Crystal structure of colicin Ia. *Nature* 385, 461-464.
- You, S., Peng, S., Lien, L., Breed, J., Sansom, M.S.P., & Woolley, G.A. (1996) Engineering stabilized ion channels: Covalent dimers of alamethicin. *Biochemistry* 35, 6225-6232.

# **Project Outputs**

## 1. Publication using data from the project:

**Krittanai**, C. and Panyim, S. A Channel-Forming Peptide from *De Novo* Design. (*Manuscript is in preparation*)

## 2. Publication associated with data or techniques established by the project:

- 2.1 Puntheeranurak, T., Leetachewa, S., Katzenmeier, G., Krittanai, C., Panyim, S. and Angsuthanasombat, C. (2001) Expression of biochemical characterization of the Bacillus thuringiensis Cry4B alpha4-alpha5 pore-forming fragment. *J. Biochem. Mol. Biol.* 34: 293-298.
- 2.2 **Kritttanai**, C., Lungchukiet, P., Ruagwetdee, S., Tuntitippawan, T., Panyim, S. and Angsuthanasombat, C. (2001) Redesign of an interhelical loop of the *Bacillus thuringiensis* Cry4B δ-endotoxin for proteolytic cleavage. *J. Biochem. Mol. Biol.* 34: 150-155
- 2.3 Jirajaroenrat, K., Pongjaroenkit, S., Krittanai, C., Prapanthadara, L. and Ketterman, A. J.(2001) Heterologous expression and characterization of alternatively spliced glutathione S-transferases from a single Anopheles gene. *Insect Biochem. Mol. Biol.* 31: 867-875.

#### 3. Poster presentation in international conferences:

- 3.1 Uawithya, P., Krittanai, C., Katzemeier, G., Leetachewa, S., Panyim, S., Angsuthanasombat, C. 3-D models for Bacillus thuringiensis Cry4A and Cry4B insecticide proteins based on homology modeling.
- In the 32<sup>th</sup> Annual Meeting of Society of Invertebrate Pathology, University of California at Irvine, August 22-27, 1999
- 3.2 Uawithya, P., Chanama, U., Potvin, L., Schwartz, J.L., Krittanai, C., Katzenmeier, G., Panyim, S. and Angsuthanasombat, C. (2000) Ion-channel formation in artificial lipid membranes by the *Bacillus thuringiensis* Cry4B toxin. *In the 44<sup>th</sup> Aannual Meeting for Biophysical Society, New Orleans, USA*. (Abstract Published in *Biophys. J.*, 78: 175.)
- 3.3 Puntheeranurak, T., Leetacheewa, S., Katzenmeier, G., Krittanai, C., Panyim S, Angsuthanasombat, C. Expression and biochemical characterisation of the Bacillus thuringiensis Cry4B A1-A5 pore-forming fragment. In the 45<sup>th</sup> Annual Meeting for Biophysical Society, Boston, USA, (Abstract published in Biophys J., 80: 585.)